Variational Method in Deriving K_0

By Farid A. Chouery[1], P.E., S.E.

Abstract

In this paper it is shown that K_0, the at rest earth pressure coefficient, can be related theoretically to failure parameters of soil (c and ϕ). The approach is to use failure mechanism that causes the soil to fail while keeping the at rest lateral pressure. Variational method is used to derive the real K_0. An approximate and a closed form derivation are obtained in sand. The approximate solution gives an equation for K_0 identical to the traditional equation by Jáky. The closed form equation shows a slightly higher K_0 value and gives a better comparison with experiments. The resulting failure surface is successfully compared to rigidly reinforced soil walls. Further analysis was done to obtain a reasonable approximation of K_0 for clay and overconsolidated sand and clay. The result shows K_0 is not constant with depth due to the cohesion. The tension zone for the at rest condition is also obtained.

Introduction and Review

The ratio of horizontal to vertical stress is expressed by a factor called the coefficient of lateral stress or lateral stress ratio and is denoted by the symbol K: $K = \sigma_h / \sigma_v$, where σ_h is the horizontal stress and σ_v is the vertical stress. This definition of K is used whether or

---

[1]Structural, Electrical and Foundation Engineer, FAC Systems Inc., 6738 19th Ave. NW, Seattle, WA

not the stresses are geostatic. Even when the stresses are static, the value of K can vary

over a rather wide range depending on whether the ground has been stretched or

compressed in the horizontal direction by either the forces of nature or the work of man.

Often the interest is in the magnitude of the horizontal static stress in the special case

where there has been no lateral strain within the ground. In the special case, the interest is

the coefficient of lateral stress at rest and uses the symbol K_0.

Sedimentary soil is built up by an accumulation of sediments from above. As this build-

up of overburden continues, there is vertical compression of the soil at any given

elevation because of the increase in vertical gravity stress. As the sedimentation takes

place, generally over a large lateral area, significant horizontal compression takes place.

Since soil is capable of sustaining internal shear stresses, the horizontal stress will be less

than the vertical stress. For a sand deposit formed in this way, K_0 will typically have a

value between 0.4 and 0.5.

On the other hand, there is evidence that the horizontal stress can exceed the vertical stress

if a soil deposit has been heavily preloaded in the past. In effect, the horizontal stresses

were "locked-in" when the soil was previously loaded by additional overburden, and did

not fully disappear when this loading was removed. For this, K_0 may reach a value of 3.

When the accumulation of sediments from above causes consolidation without locked-in

stresses, it is referred to as "normal consolidation". The problem of normally consolidated

sand under a widely loaded area has been theoretically investigated by Jáky, (1944, 1948) [10,11], and Handy, (1985) [8], yielding

$$K_0 = 1 - \sin\phi \quad\text{...}\quad (1)$$

where ϕ is the angle of internal friction of the soil. The original derivation of Jáky gives a more complicated expression that he approximated by $K_0 = 0.9 - \sin\phi$ [10], and later simplified it to equation 1[11]. Handy shows that if instead of using a flat arch, he had used a catenary, the examination indicates $K_0 = 1.06(1 - \sin\phi)$ [8]. He mentioned that neither of these derivations is consistent with the common use of K_0 to define the stress ratio in normally consolidated soil under a widely loaded area, as mentioned above, the agreement with experimented data, well investigated by Mayne and Kulhawy, (1982) [17], being defined as coincidence[9]. Similarly, Tschebotarioff, (1953) [28], commented that Jáky's assumptions in the derivation[9] are unacceptable. Handy [8] gave also a mathematical proof, (Eq. 11 of his paper), in which Jáky's equation can be derived using the approximate vertical stress. His final recommendation is to use $K_0 = 1.1(1 - \sin\phi)$ as a safer approximation, since the equation for K_0 originally derived from a consideration of arching, and for an immobile, rough wall. Practicing engineers can be unaware of these finer distinctions in theoretical and experimental considerations, and use K_0 of Eq. 1 routinely.

In this paper variational method, reference [29], is used first to derive K_0 for normal and overconsolidated sand. The method is applied over a soil failure mechanism the keeps the

at rest lateral forces unchanged. Second: a reasonable approximation is derived for normal and overconsolidated clay. Also, rigid reinforced soil is examined for comparing the derived slip surfaces. The derivation can be readily extended for a slanted wall with a sloped soil on surface. This in turn prepares the way for dynamic analysis.

Incipient Shear and K_0 Failure Mechanism

Consider taking a horizontal slice from the ground with a height y, and introducing an imbalance loading as seen in Fig. 1(a). Assume that the soil was at the at rest condition before introducing the imbalance surcharge loads. It is desirable to show the effect of this imbalance loading on the horizontal force on line A-B. Thus, we need to investigate the loads before and after the imbalance loading. (1) <u>Before:</u> By taking an arbitrary angle α to create two immobilized wedges, as seen in Fig. 1(a), the sum of the forces yields:

$E_h = N \sin\alpha - F \cos\alpha$, and $W = N \cos\alpha + F \sin\alpha$, where W is the weight of the wedge, E_h is the horizontal force on line A-B, N is the normal force, and F is the immobilized friction. (2)<u>After:</u> By using the same arbitrary angles, the change in N and F, due to the imbalance surcharge loading q and - q, is ΔN and ΔF respectively. When considering axi-symmetry, the net change ΔN and ΔF on one wedge is equal and opposite to the net change on the other wedge. From Fig. 1(b) the new equations yields: (1) the right wedge (ABD): $-\Delta N \cos\alpha - \Delta F \sin\alpha = -qy \cot\alpha - T$, and $\Delta E_h = -\Delta N \sin\alpha + \Delta F \cos\alpha$. (2) the left wedge (ABC): $\Delta N \cos\alpha + \Delta F \sin\alpha = qy \cot\alpha + T$, and $\Delta E_h = \Delta N \sin\alpha - \Delta F \cos\alpha$. Equating ΔE_h from the left wedge to the right wedge yields $\Delta F = \Delta N \tan\alpha$. When substituting back to find ΔE_h, it gives $\Delta E_h = 0$. Thus the imbalance loading does not change the at rest force on line A-B where the maximum shear occurs. If the surcharge

pressure q and $-q$ is continually increased the result is a failure surface, where $\Delta F + F$ in the left wedge (ABC) reaches the failure criterion of a fully mobilized friction. For the right wedge (ABD), the friction will not quite be fully mobilized. To show this, it is sufficient to show that $(F + \Delta F) / (N + \Delta N) > (F - \Delta F) / (N - \Delta N)$. This lead to $\Delta F / \Delta N > F / N$, or $\tan \alpha > \tan \alpha - E_h / (N \cos \alpha)$, which is true.
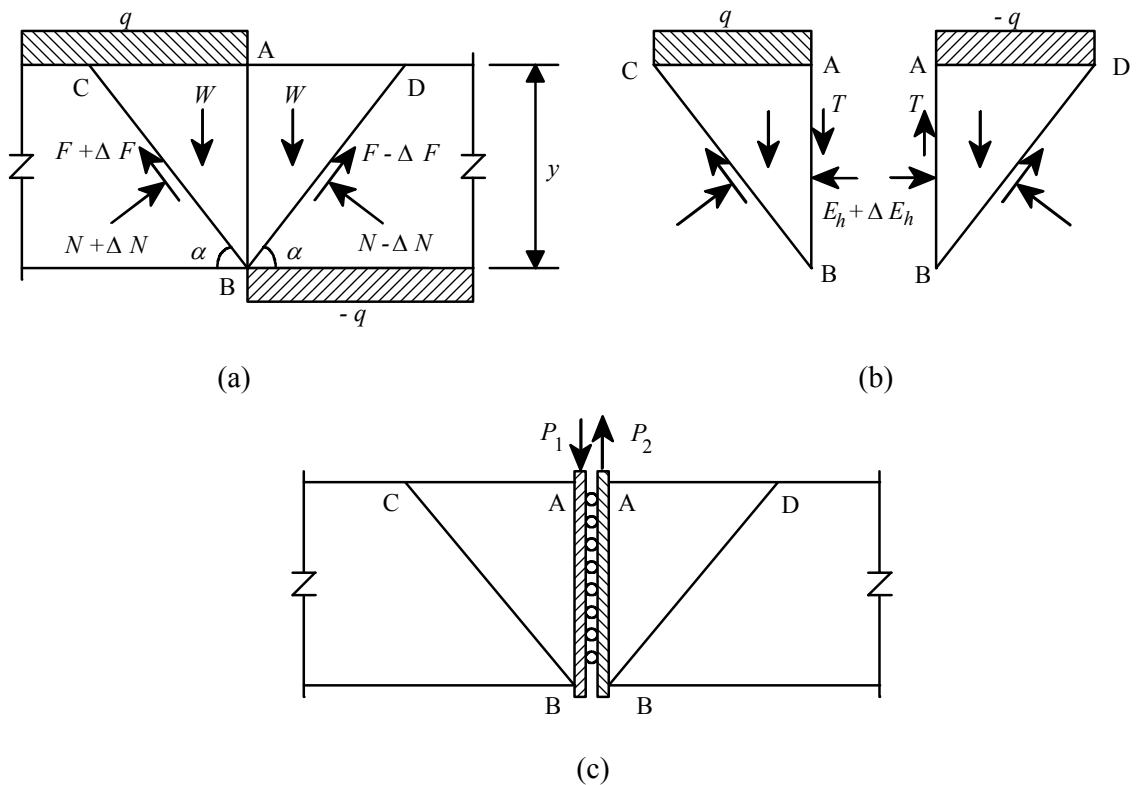
FIG. 1 - Incipient Shear Definitions (a) Horizontal Slice (b) Force Diagram
(c) Incipient shear on two sliding walls.

A reasonable question: if the failure surface is not a line, will it change ΔE_h? If the above analysis was to assume a curve instead of a line for the immobile friction, the hypothesis ($\Delta E_h = 0$) would still hold for the right and left vertical slices adjacent to line A-B. This

can be seen by treating the bottom of each slice as a wedge with some slope and a surcharge on top of it. Repeating the analysis on each slice with its corresponding mirror image slice, will give the same results, when summing all the forces. Thus, the hypothesis is valid for any arbitrary curve, and not just a line. Furthermore, if the imbalance loading q and - q were any axi-symmetric loading, the hypothesis that $\Delta E_h = 0$ remains valid. From this observation it is necessary to introduce a name for the type of shear, T, which was introduced on line A-B to be the *incipient shear*. The full definition of the incipient shear is: *A shear introduced to a boundary or a line is an incipient shear when the normal forces to the boundary or the line do not change*. It is important to note that the horizontal force of Fig. 1(a) does not need to be the at rest force. Thus, the incipient shear hypothesis is applicable for other conditions.

It is noteworthy that the hypothesis of the incipient shear was arrived at without the use of elasticity, plasticity, or elastoplastic methods. When comparing with elasticity the result is the same. For example, integrating Flamant's equation, (1892) [27], for any axi-symmetric load on a semi-infinite media yields $\sigma_h = \sigma_v = 0$, and the strain is zero at line A-B of Fig. 1(a).

To simplify the analysis it would be beneficial not to deal with the surcharge q. Consider the two buried walls in the horizontal slice of Fig. 1(c). Between the walls are rollers to give a perfectly smooth surface. If $P_1 = P_2$, the wedge analysis is identical to the above for Fig. 1(a). The result is the same hypothesis $\Delta E_h = 0$. The first failure surface would be that of P_1, a downward incipient shear. The failure surface is expected to be different than

6

that of Fig. 1(a). However, the before and after, at rest lateral forces are kept the same since $\Delta E_h = 0$.

From these observations, when considering the downward incipient shear of Fig. 1(c), it is expected that the K value will have variation inside the wall. It will start at $K = K_0$ at the wall and will reoccur internally at some distance inside the wall. This is necessary since going further inside the wall, the incipient shear has a lesser influence on the stresses and the at rest forces will reoccur. Thus K_0 will reoccur at some point at $x = x_m$ from the wall and the boundary condition on the slip surface can be considered to have K_0 at both ends.

Once the K_0 failure mechanism is realized, K_0 can be derived from finding the maximum horizontal force for an active slip surface. Additionally, the boundary condition must be satisfied. Maximizing the horizontal force will lead to K_0, and not any other active force coefficient because the horizontal force will reduce if the boundary moves slightly outward from zero deformation to an active slip surface. Experiments by Terzaghi (1934, 1941) [25, 26], Sherif et al. (1982,1984) [21, 23], and Fang et al. (1986) [7] indicated that regardless of the outward movement of a rigid wall, the horizontal force reduces from the at rest condition. Thus, the at rest force is the upper bound for an active slip surface failure. These tests were done for translating walls, rotating walls from top and bottom. The outward movement reduces the horizontal force from the at rest condition because it induces tension in the soil. Cohesionless soil can hardly take tension. Thus, if the failing wedge is subdivided into vertical slices, the shear in the slices will reduce. Excessive

outward movement will result in an active condition where the shear in the slices

becomes zero. Hence, it is sufficient to find the at rest force by maximization with an

active slip surface due to a downward incipient shear with the proper boundary condition.

Thus the necessary criterion in deriving K_0 is obtained.

Boundary Conditions for Sand

Subdividing the failure wedge of the downward incipient shear into vertical slices,

following Bishop (1955) [1], yields slices that are each in equilibrium, so that the

overturning moments remain in balance and not of concern. Each slice is added together

to make the wedge in Fig. 2. The resultant of the boundary forces on a slice can be

transformed to a Coulomb, (1776) [3], wedge as shown on Fig. 3(a),(b). From the

Coulomb wedge one can write

$$dE_x = \frac{\tan(\alpha - \phi)}{1 + \tan\delta \tan(\alpha - \phi)} \left(\frac{d\overline{w}}{\tan\alpha} \right) , \dots\dots\dots\dots\dots\dots\dots\dots\dots\dots\dots\dots\dots \text{(2)}$$

$$dW = -\gamma \left[\frac{(y - dy) + y}{2} \right] \frac{dy}{\tan\alpha} = \frac{d\overline{w}}{\tan\alpha} , \dots\dots\dots\dots\dots\dots\dots\dots\dots\dots\dots \text{(3)}$$

$$dE_y = dE_x \tan\delta , \dots\dots\dots\dots\dots\dots\dots\dots\dots\dots\dots\dots\dots\dots\dots\dots\dots\dots \text{(4)}$$

and

$$dy = -dx \tan\alpha \dots\dots\dots\dots\dots\dots\dots\dots\dots\dots\dots\dots\dots\dots\dots\dots\dots\dots\dots \text{(5)}$$

Extremizing the boundary forces in a slice can be done in three ways: (1) extremizing the

horizontal force dE_x , (2) extremizing the vertical force dE_y , (3) extremizing the resultant

force of dE_x and dE_y. To extremize dE_x it is necessary to hold dy constant and vary dx

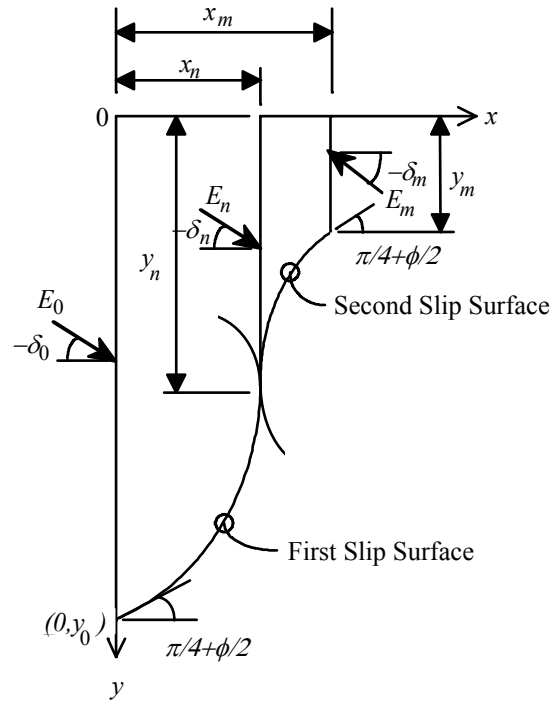because $dE_x = -Kydy$, and extremizing K is of interest. Thus ydy must be
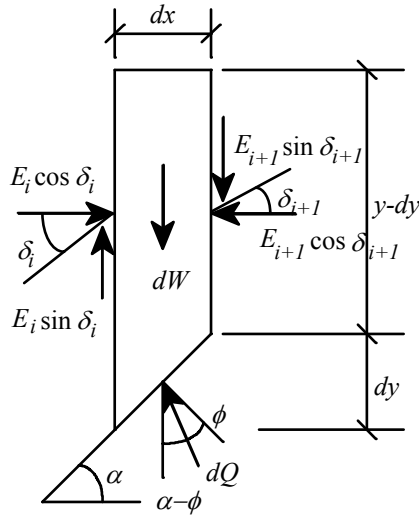
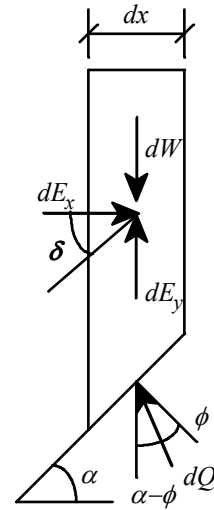FIG. 2- Slip Surfaces Due To Incipient Shea

FIG. 3-a Bishop Slice   FIG. 3-b Coulomb Wedge

held constant. To extremize dE_y dx must be held constant and dy must be varied. dE_y must be extremized to achieve a constant $dW = \gamma y dx$. Thus, ydx must remain constant. In many cases, dE_y is taken as $dE_x \tan\delta$. In these cases dy is to be held constant and dx is to vary. To extremize the resultant it requires $dx \tan(\alpha - \delta) / \cos\delta$ be held constant. This can be realized by rotating the axis by δ from the vertical in order to have the resultant in a horizontal direction.

In the boundaries in Fig. 2, it is desirable to find the angle α that gives the smallest dE_y, which causes the first and last slice to fail, while dE_x is at maximum. From the above consideration on extremizing the forces in a slice, one finds that dx and dy must be held constant. This gives no unique solution since two different α's can be derived from Eq. 5. However, at the boundaries the forces are already at maximum and $dE_x = K_0 \gamma y dy$

regardless of α or the value of the incipient shear. Additionally, the bulk of the movement

is in the vertical direction. Thus the failure of these slices will be primarily from dE_y due

to the incipient shear. Therefore the slice wedge at the boundaries can be considered to

have movements in the vertical direction, and α can be obtained by keeping only dx

constant. Writing Eq. 2 in terms of dE_x and dE_y with Eq. 5 and Eq. 3, yields

$$-dE_y = -\gamma \frac{[(y-dy)+y]}{2}dx + dE_x \cot(\alpha - \phi) = -\gamma y dx + (\gamma K_0 y dx)\tan\alpha\cot(\alpha - \phi) \;\text{........ (6)}$$

Minimizing the downward force $-dE_y$ in Eq. 6, $-\dfrac{dE_y}{d\alpha}\bigg|_{x=0 \text{ and } x=x_m} = 0$, yields

$$\alpha = \alpha_0 = \alpha_m = \pi/4 + \phi/2 \;\text{.. (7)}$$

where α_0 is the wedge angle for the first slice, and α_m is for the last slice. Note: $\alpha = 0$ is

not considered as solution for the minimum of Eq. 6, since the downward movement will

cause a non-zero slope in the slices. Also, $\alpha = \pi/2 + \phi$ cannot be considered as a solution

since $\alpha \le \pi/2$. Now that the boundary conditions are selected, maximizing the horizontal

force with these boundaries must result in K_0. A first approximation can be done by

selecting the slip surface as a line with a slope at all α's in the slices to be $\pi/4 + \phi/2$,

and selecting $\delta = -\phi$ to maximize the horizontal force in Eq. 2. Substituting

$\alpha = \pi/4 + \phi/2$, and $\delta = -\phi$ in Eq. 2 and integrating y from y_0 to zero yields

$$E_0 \cos\delta_0 = \int dE_x \cong -\gamma \int_{y_0}^{0} \frac{\tan(\pi/4 - \phi/2)}{1 - \tan\phi\tan(\pi/4 - \phi/2)} \frac{1}{\tan(\pi/4 + \phi/2)} y\,dy$$

11

$$\cong \frac{\gamma y_0{}^2}{2}(1 - \sin\phi) \quad \text{...} \quad (8)$$

where the identity $\tan(\pi/4 \pm \phi/2) = \pm\tan\phi + 1/\cos\phi$ were used. Eq. 8 gives a

$K_0 \cong 1 - \sin\phi$ as in Eq. 1, where Jáky's equation is derived from unacceptable

assumptions and is considered a coincidence. There are considerations that need to be

investigated for this approximation: (1) The integration of Eq. 4 yields $\delta_0 = -\phi$. However,

another slip surface can occur before this one, where the incipient shear is lower and

reaches a directional angle $-\delta_0 < \phi$ with a slightly higher K_0 value than Eq. 8. This will be

shown later on in the derivation. (2) Eq. 8 is derived by assuming a constant K_0 value in

all the slices. This is contrary to common sense since variation in the stresses, thus the K

value, are expected inside the wall. It can be concluded that Eq. 8 or Jáky's equation is

only an approximation, and the slip surface and the directional angle δ_0 are incorrect.

Sand Analysis

K_0 for sand will be derived from an extremum condition using variational methods with

the boundary condition of Eq. 7. With the extremum method one selects arbitrary

admissible slip surfaces and determines the forces acting on the boundaries of the earth

mass. The definitive slip surface is one, which furnishes an extremum value for the

horizontal force. Maximizing the horizontal force $E_0 \cos\delta_0$ can start by maximizing each

slice individually. The horizontal force dE_x of the slice in Eq. 2 can be treated as a

coulomb wedge with a uniform surcharge; it is required that $\dfrac{dE_x}{d\alpha} = 0$. Thus

$$\tan\delta = \left[\frac{\sin 2\alpha}{\sin 2(\alpha-\phi)} - 1\right]\frac{1}{\tan(\alpha-\phi)} = \frac{\cos(2\alpha-\phi)\sin\phi}{\sin^2(\alpha-\phi)} = \frac{(\cot^2\alpha-1)\cot\phi+2\cot\alpha}{(\cot\phi-\cot\alpha)^2}$$

.... (9)

where $\tan\delta$ is expressed three different ways for convenience and it yields

$$\cot\alpha = -\tan(\delta+\phi)\left[1 - \sqrt{1+\cot(\delta+\phi)\cot\phi}\right] \quad .... (10)$$

If plotting Eq. 10 it shows that $\alpha > \phi$ for all $-\phi \le \delta \le \phi$. Also, Eq.10 is the Coulomb

wedge angle for a vertical wall with wall friction. If $\delta = 0$ in Eq. 9 or 10 $\alpha =$

$\pi/4 + \phi/2$, where $-\tan\phi + 1/\cos\phi = \cot(\pi/4+\phi/2)$. This checks with an active

Coulomb wedge with $\delta = 0$. Now, note for $\alpha > \phi$ in Eq. 2 the force dE_x is maximized

when $\delta \le 0$. Thus the boundary points for the slip surface of Fig. 2 can be taken in the

region $-\phi \le \delta \le 0$ or at $\pi/4 + \phi/2 \le \alpha \le \pi/2$. Thus, $\alpha_0 = \pi/4 + \phi/2$, and $\alpha_n = \pi/2$ as in Eq. 7.

For a given y_0, x_n and y_n will be determined from these prescribed end points. Substituting

Eq. 9 in Eq. 2 and 4 and rearranging yields

$$dE_x = \gamma\sin^2\phi(\cot\phi-\cot\alpha)^2\tan\alpha ydx \quad .... (11)$$

$$dE_y = 2\gamma\sin^2\phi ydx + \gamma\sin\phi\cos\phi(\cot\alpha-\tan\alpha)ydx$$

$$= -\gamma\tan\phi\tan\alpha ydx + \gamma\cos\phi\sin\phi(\tan\phi+\cot\alpha)^2\tan\alpha ydx$$

$$= \tan\phi(\gamma\cot\alpha ydx - dE_x) \quad .... (12)$$

Where $\dfrac{dw}{\tan\alpha}$ is replaced by γydx, γ is the soil constant, and dE_y is expressed in different

ways for convenience. From Fig. 3a one can write

13

$$E_i \cos\delta_i - E_{i+1} \cos\delta_{i+1} = dE_x \quad \text{.. (13)}$$

$$E_i \sin\delta_i - E_{i+1} \sin\delta_{i+1} = dE_y \quad \text{.. (14)}$$

When starting with E_0 and ending with E_n Eqs. 13 and 14 yields

$$E_0 \cos\delta_0 = \sum_{i=0}^{n-1} dE_x + E_n \cos\delta_n \quad \text{.................................... (15)}$$

$$E_0 \sin\delta_0 = \sum_{i=0}^{n-1} dE_y + E_n \sin\delta_n \quad \text{.................................... (16)}$$

By taking $\tan\alpha = -y'$ in Eq. 11 and 12 and replacing the summation sign by the integral sign in Eq. 15 and 16 it yields

$$E_0 \cos\delta_0 = -\gamma \sin^2\phi \int_0^{x_n} \left(\cot\phi + \frac{1}{y'}\right)^2 y'y\,dx + E_n \cos\delta_n \quad \text{................................... (17)}$$

$$E_0 \sin\delta_0 = 2\gamma \sin^2\phi \int_0^{x_n} y\,dx + \gamma \sin\phi\cos\phi \int_0^{x_n} \left(y' - \frac{1}{y'}\right) y\,dx + E_n \sin\delta_n$$

$$= \gamma \tan\phi \int_0^{x_n} y'y\,dx - \gamma \sin\phi \cos\phi \int_0^{x_n} \left(\tan\phi - \frac{1}{y'}\right)^2 y'y\,dx + E_n \sin\delta_n$$

$$= -\gamma \tan\phi \int_0^{x_n} \frac{y}{y'}\,dx - \gamma \tan\phi \int_0^{x_n} dE_x + E_n \sin\delta_n \quad \text{........................... (18)}$$

To use variational method to maximize horizontal force $E_0 \cos\delta_0$, Eq. 17 needs to be extremized while Eq. 18 is to be satisfied. Eq. 18 can be satisfied by choosing the proper

directional angles δ_0 and δ_n. Similarly, $E_0 \cos \delta_0$ can be maximized by extremizing Eq. 18 while Eq. 17 to be satisfied, and again the proper directional angles can satisfy Eq. 17. Note: $E_0 \sin \delta_0$ is taken as $(E_0 \cos \delta_0) \tan \delta_0$. These conditions leads to a deduction that there are two slip surfaces that can maximize $E_0 \cos \delta_0$, and both surfaces can occur. Since it is desirable to look for the horizontal pressure in Fig. 2, the resulting slip surface from maximizing Eq. 17 will be the first slip surface and the slip surface resulting from maximizing Eq. 18 will be the next one. This situation will become more evident when the slip surfaces are obtained and the boundary conditions are imposed. Thus, Eq. 17 or 18 can be extremized alone while the other can be satisfied with a suitable δ_0 and δ_n.

When starting with Eq. 17 the boundary conditions are prescribed: at $x = 0$ $y = y_0$, at $x = 0$ and $y = y_0$ $x' = -\tan(\pi/4 - \phi/2) = \tan \phi - 1/\cos \phi$, and at $x = x_n$ and $y = y_n$ $x' = 0$. Note also that $E_n \cos \delta_n$ in Eq. 17 is prescribed from a second slip surface such that $\delta(E_n \cos \delta_n) = 0$. Thus, the Euler equation [29] from variational method can be applied:

$$\frac{\partial \Re}{\partial y} - \frac{d}{dx}\left(\frac{\partial \Re}{\partial y'}\right) = 0 \quad \text{...} \quad (19)$$

$$\text{where} \quad \Re = -\gamma \sin^2 \phi \left(\cot \phi + \frac{1}{y'}\right)^2 y'y \quad \text{...} \quad (20)$$

Since $\Re$ does not involve x explicitly then

$$\Re - y'\frac{\partial \Re}{\partial y'} = h \quad \text{..} \quad (21)$$

where h is a constant. Applying Eq. 21 on Eq. 20 yields

$$\frac{1}{y'} = -\cot\phi\left(1 - \frac{h'}{y}\right) \quad \text{... (22)}$$

where h' is a new constant. By using the boundary condition $x' = 0$ at $y = y_n$, h' can be

found and Eq. 22 can be written as

$$\frac{1}{y'} = x' = -\cot\phi\left(1 - \frac{y_n}{y}\right) \quad \text{... (23)}$$

By using the end condition at $y = y_0$ $\quad x' = \tan\phi - 1/\cos\phi \quad$ for $\alpha_0 = \pi/4 + \phi/2$ on Eq.

23 yields

$$y_0 = (1 + \sin\phi)y_n \quad \text{... (24)}$$

When integrating Eq. 23 and using the end condition at $x = 0$ $y = y_0$, it yields the first

slip surface Eq.:

$$x = -\cot\phi\left[y - y_0 - y_n \ln\left|\frac{y}{y_0}\right|\right] \quad \text{.. (25)}$$

By using Eq. 24, Eq. 25 can be written as

$$\Omega = \frac{\cot\phi}{1 + \sin\phi}\left[-(1 + \sin\phi)(\psi - 1) + \ln\psi\right] \quad \text{... (26)}$$

Where $\Omega = \dfrac{x}{y_0}$ and $\psi = \dfrac{y}{y_0}$. Fig. 4 shows different slip surfaces for various values of ϕ

for the region $\dfrac{1}{1 + \sin\phi} < \psi < 1$. The horizontal distance can be written as

$$x_n = \frac{y_0 \cot\phi}{1 + \sin\phi}\left[\sin\phi + \ln(1 + \sin\phi)\right] \quad \text{... (27)}$$
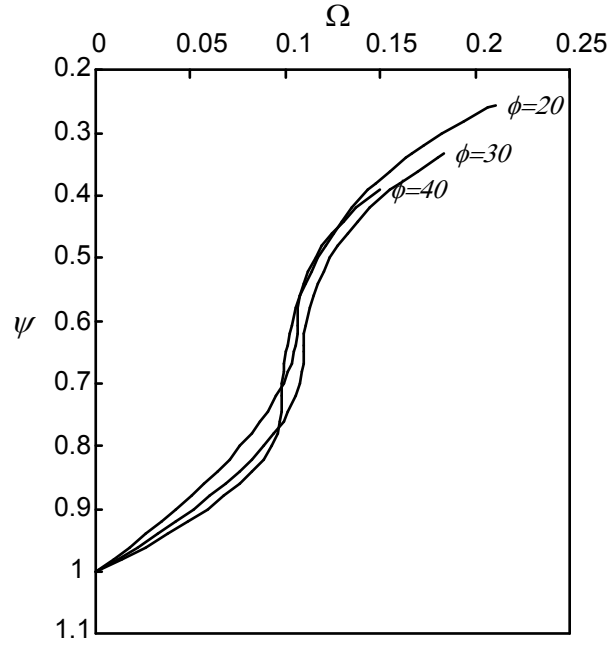
16

FIG. 4 K_0 First Slip Surface

By substituting Eq. 23 in Eq. 17 and 18, changing the interval to $[y_0, y_n]$ instead of

$[0, x_n]$, and replacing $y'dx$ by dy, yields

$$E_0 \cos \delta_0 = -\gamma \sin^2 \phi \int_{y_0}^{y_n} \frac{y_n^2 \cot^2 \phi}{y} dy + E_n \cos \delta_n$$

$$= \gamma y_n^2 \cos^2 \phi \ln \left| \frac{y_0}{y_n} \right| + E_n \cos \delta_n \quad .... \text{(28)}$$

$$E_0 \sin \delta_0 = \frac{\gamma \cot \phi}{2} (y_n - y_0)(3y_n - y_0) + \gamma y_n^2 \cot \phi \cos^2 \phi \ln \left| \frac{y_0}{y_n} \right| + E_n \sin \delta_n \quad .... \text{(29)}$$

17

Substituting Eq. 24 in Eq. 28 and 29 yields

$$E_0 \cos\delta_0 = \gamma y_n^2 \cos^2\phi \ln(1+\sin\phi) + E_n \cos\delta_n \quad\text{.. (30)}$$

$$E_0 \sin\delta_0 = -\gamma \frac{y_n^2 \cos\phi}{2}(2-\sin\phi) + \gamma y_n^2 \cot\phi\cos^2\phi \ln(1+\sin\phi) + E_n \sin\delta_n \quad\text{............... (31)}$$

Thus the analysis of the first slip surface is obtained. Note for $x > x_n$ Eq. 23 has no y values. In fact the curve circles toward the first boundary, as seen in Fig. 2, indicating another slip surface must occur in order to reach the top of the ground. So, it remains to find the second slip surface and the force E_n. Consider the second slip surface shown in Fig. 2.

For maximum condition in the slice using Eq. 2 and for matching the end of the first slip surface, the boundary condition can be taken as $\alpha_n = \pi/2$ and $\alpha_m = \pi/4 + \phi/2$.

Rewriting Eq. 17 and 18 in terms of the forces of the second slip surface in Fig. 2, yields

$$E_n \cos\delta_n = -\gamma\sin^2\phi \int_{x_n}^{x_m}\left(\cot\phi + \frac{1}{y'}\right)^2 y'y\,dx + E_m \cos\delta_m \quad\text{.. (32)}$$

$$E_n \sin\delta_n = \gamma\tan\phi \int_{x_n}^{x_m} y'y\,dx - \gamma\sin\phi\cos\phi \int_{x_n}^{x_m}\left(\tan\phi - \frac{1}{y'}\right)^2 y'y\,dx + E_m \sin\delta_m \quad\text{.................. (33)}$$

Using variational method on Eq. 33 to extremize $E_n \cos\delta_n$ yields

$$x' = \tan\phi\left(1 - \frac{h'}{y}\right) \quad\text{.. (34)}$$

where h' is a constant. By using the boundary condition at $y = y_n$ $x' = 1/y' = 0$ for

$\alpha_n = \pi/2$ on Eq. 34, h' is found and the equation can be rewritten as

$$x' = \tan\phi\left(1 - \frac{y_n}{y}\right) \quad\text{..} \quad (35)$$

Using the other end condition at $y = y_m$ $x' = \tan\phi - 1/\cos\phi$ for $\alpha_m = \pi/4 + \phi/2$, Eq. 35 yields

$$y_m = y_n \sin\phi \quad\text{...} \quad (36)$$

When integrating Eq. 35 and using the end condition at $x = x_n$ $y = y_n$, the second slip surface is obtained:

$$x = \tan\phi\left(y - y_n - y_n \ln\left|\frac{y}{y_n}\right|\right) + x_n \quad\text{..} \quad (37)$$

From Eq. 24, 27 and 36, Eq. 37 can be rewritten as

$$\Omega = \frac{1}{1+\sin\phi}\left\{\tan\phi\left[(1+\sin\phi)\psi - 1 - \ln\left[(1+\sin\phi)\psi\right]\right] + \cot\phi\left[\sin\phi - \ln(1+\sin\phi)\right]\right\} \text{........} (38)$$

Where $\Omega = \dfrac{x}{y_0}$, $\psi = \dfrac{y}{y_0}$, and $\dfrac{\sin\phi}{1+\sin\phi} < \psi < \dfrac{1}{1+\sin\phi}$, see Fig. 4 for the plot of Ω and

ψ for the second slip surface. The total horizontal distance can be written as

$$x_m = \frac{y_0}{1+\sin\phi}\left\{\tan\phi\left[\sin\phi - 1 - \ln(\sin\phi)\right] + \cot\phi\left[\sin\phi - \ln(1+\sin\phi)\right]\right\} \text{...........................} (39)$$

19

By substituting Eq. 35 in Eq. 32 and 33 with the interval $[y_n, y_m]$ instead of $[x_n, x_m]$ and with $y'dx = dy$, it yields

$$E_n \cos \delta_n = \gamma y_n{}^2 \left\{ \frac{1}{2\cos^2 \phi}\left[1-\left(\frac{y_m}{y_n}\right)^2 \right] - 2\tan^2 \phi\left[1-\frac{y_m}{y_n} \right] - \tan^2 \phi\sin^2 \phi\ln\left|\frac{y_m}{y_n}\right| \right\} + E_m \cos \delta_n$$

.... (40)

$$E_n \sin \delta_n = \gamma y_n{}^2 \left\{ -\frac{\tan \phi}{2}\left[1-\left(\frac{y_m}{y_n}\right)^2 \right] - \tan \phi\sin^2 \phi\ln\left|\frac{y_m}{y_n}\right| \right\} + E_m \sin \delta_m \quad \text{......................... (41)}$$

Substituting Eq. 36 in Eq. 40 and 41 yields

$$E_n \cos \delta_n = \gamma y_n{}^2 \left[\frac{1}{2} - 2\tan^2 \phi(1-\sin \phi) - \tan^2 \phi\sin^2 \phi\ln(\sin \phi) \right] + E_m \cos \delta_m \quad \text{................ (42)}$$

$$E_n \sin \delta_n = -\gamma y_n{}^2 \left[\frac{\sin \phi\cos \phi}{2} + \tan \phi\sin^2 \phi\ln(\sin \phi) \right] + E_m \sin \delta_m \quad \text{................................. (43)}$$

Substituting Eq. 42 and 43 in Eq. 30 and 31 yields

$$E_0 \cos \delta_0 = \gamma y_n{}^2 \left[\cos^2 \phi\ln(1+\sin \phi) + \frac{1}{2} - 2\tan^2 \phi(1-\sin \phi) - \tan^2 \phi\sin^2 \phi\ln(\sin \phi) \right] + E_m \cos \delta_m$$

.... (44)

$$E_0 \sin \delta_0 = \gamma y_n{}^2 \left[-\frac{\cos \phi}{2}(2-\sin \phi) + \cot \phi\cos^2 \phi\ln(1+\sin \phi) - \frac{\sin \phi\cos \phi}{2} - \tan \phi\sin^2 \phi\ln(\sin \phi) \right] + E_m \sin \delta_m$$

.... (45)

Now Eq. 44 and 45 gives the maximum possible $E_0 \cos \delta_0$ for the given boundary

conditions. Since the boundary conditions are satisfied, the horizontal forces can be taken

as $E_0 \cos \delta_0 = \gamma K_0 \dfrac{y_0^{\,2}}{2}$, and $E_m \cos \delta_m = \gamma K_0 \dfrac{y_m^{\,2}}{2}$ in Eq. 44. Thus, from Eq. 44, 24, and

36 K_0 can be found:

$$K_0 = \frac{2\cos^2 \phi \ln(1+\sin \phi) + 1 - 4(1-\sin \phi)\tan^2 \phi - 2\tan^2 \phi \sin^2 \phi \ln(\sin \phi)}{(1+\sin \phi)^2 - \sin^2 \phi} \quad \text{............... (46)}$$

Since δ_0 and δ_m are arbitrary, they can be set equal. This can be realized since the

incipient shear can be assumed to vary linearly with depth at the boundaries. Thus, from

Eq. 45, setting $E_0 \sin \delta_0 = E_0 \cos \delta_0 \tan \delta_0 = \gamma K_0 \dfrac{y_0^{\,2}}{2}\tan \delta_0$ and

$E_m \sin \delta_m = E_m \cos \delta_m = \gamma K_0 \dfrac{y_m^{\,2}}{2}\tan \delta_0$, it yields the incipient shear directional angle:

$$\tan \delta_0 = \tan \delta_m = \frac{-\cos \phi(2-\sin \phi) + 2\cot \phi \cos^2 \phi \ln(1+\sin \phi) - \sin \phi \cos \phi - 2\tan \phi \sin^2 \phi \ln(\sin \phi)}{\left[(1+\sin \phi)^2 - \sin^2 \phi\right]K_0}$$

$$\text{.. (47)}$$

From Eq. 30 and 31 $\tan \delta_n$ can be expressed as:

$$\tan \delta_n = \frac{E_0 \sin \delta_0 + \gamma y_n^{\,2}\cos \phi(2-\sin \phi)/2 - \gamma y_n^{\,2}\cot \phi \cos^2 \phi \ln(1+\sin \phi)}{E_0 \cos \delta_0 - \gamma y_n^{\,2}\cos^2 \phi \ln(1+\sin \phi)} \quad \text{............... (48)}$$

or

$$\tan \delta_n = \frac{K_0(1+\sin \phi)^2 \tan \delta_0 + \cos \phi(2-\sin \phi) - 2\cot \phi \cos^2 \phi \ln(1+\sin \phi)}{K_0(1+\sin \phi)^2 - 2\cos^2 \phi \ln(1+\sin \phi)} \quad \text{............... (49)}$$

Table 1 gives the comparison of different K_0 for Jáky, Handy, and as derived. Note $-\delta_0 < \phi$ for all ϕ and the incipient shear is smaller indicating that K_0 of Eq. 46 supersedes that of Eq. 8.

Due to the propagation of the incipient shear, it can be anticipated that the two slip surfaces can repeat for $x > x_m$. Now, it is important to show that the K_0 of Eq. 46 is the same when considering all the slip surfaces to the top of the ground. Let K_1 be the term in the bracket of Eq. 44. Utilizing Eqs. 24 and 36, an expression from one set of slip surfaces to another can be obtained: $y_n(\text{bot}) / y_n(\text{top}) = \sin\phi / (1 + \sin\phi)$. Using this relation and substituting all sets of slip surfaces in Eq. 44 yields

$$E_0 \cos\delta_0 = \gamma K_1 y_n^2 \left[1 + \left(\frac{\sin\phi}{1+\sin\phi} \right)^2 + \left(\frac{\sin\phi}{1+\sin\phi} \right)^4 + \left(\frac{\sin\phi}{1+\sin\phi} \right)^6 + \cdots \right] \dots\dots\dots \quad (50)$$

or

$$E_0 \cos\delta_0 = \gamma K_1 y_n^2 \sum_{i=0}^{\infty} \left(\frac{\sin\phi}{1+\sin\phi} \right)^{2i} = \frac{\gamma K_1 y_n^2 (1+\sin\phi)^2}{(1+\sin\phi)^2 - \sin^2\phi} = \frac{\gamma K_0 y_0^2}{2} \dots\dots\dots\dots \quad (51)$$

This gives exactly the same K_0 of Eq. 46. Thus, the solution is consistent, and this method of substitution can also be done on Eq. 45 to show that $\tan\delta_0$ is exactly the same as that of Eq. 47. Consequently, the assumption that $\delta_0 = \delta_m$ is correct.

ϕ	Jáky	Jáky	Handy	Handy	Derived	$\delta_0 = \delta_m{}^*$	$\delta_n{}^*$
Deg.	1-sinϕ	0.9-sinϕ	1.1(1-sinϕ)	1.06(1-sinϕ)	K_0	Deg.	Deg.
***0	1.0000	0.9000	1.1000	1.0600	1.0000	0.00	-0.00
10	0.8264	0.7264	0.9090	0.8759	0.8989	-8.90	-9.58
20	0.6580	0.5580	0.7238	0.6975	0.7150	-16.67	-18.37
30	0.5000	0.4000	0.5500	0.5300	0.5285	-24.36	-26.74
40	0.3572	0.2572	0.3929	0.3786	0.3648	-32.51	-35.06
50	0.2340	0.1340	0.2574	0.2480	0.2311	-41.54	-43.72
60	0.1340	0.0340	0.1474	0.1420	0.1287	-51.77	-53.18
70	0.0603	-0.0397	0.0663	0.0639	0.0567	-63.38	-63.97
80	0.0152	-0.0848	0.0167	0.0161	0.0141	-76.29	-76.38
**90	0.0000	-0.1000	0.0000	0.0000	0.0000	-90.00	-90.00

* Derived in this paper.   ** As in completely rigid.   *** As in hydrostatic.

Table 1- K_0 comparison

Comparing K_0 sand with experiments

Mayne and Kulhawy, (1982) [17], made a statistical analysis of 171 tests, where some of

these tests had missing ϕ values (some in clay and some in sand). Their result showed that

Jáky's equation is applicable. However, the linear regression was biased toward curve

fitting Jáky's equation. Their correlation number $r = 0.802$ for 121 points. Adding 17

more tests, see reference [4, 5, 6, 15, 16, 18, 19, 20], and computing the absolute value of the error on 138 tests yields:

Error	Derived	Jáky
0 to 1%	23	18
1 to 5%	58	70
5 to 16%	57	50
Total No. of tests	138	138

It is clear from this observation that the derived K_0 compares with experiments just as good, perhaps a little better.

Comparison of the slip surface for sand with experiments

There is no available experimental data publication on slip surfaces for K_0 due to shear failure. However, it is notable that the slip surfaces are similar results to slip surfaces of rigid reinforced earth problems. In the reinforced soil walls (rigid type), the developments of the force $E_0 \cos \delta_0$ and $E_0 \sin \delta_0$ are dissipated in the reinforcements. Thus dE_x and dE_y in every slice are reduced by the tension of each segment in the reinforcements, ending with $E_0 = 0$ at the face of the wall. The problem of maximization has the same equations as the rigid wall. In this case, the forces in the reinforcements need to be maximized instead of the force on the boundaries. Thus, $\sum dE_x$ and $\sum dE_y$ needs to be maximized, where the slice of Fig. 3(a) and (b) will have reinforcements sticking out of it and dE_x and dE_y represent the resultant forces. Thus, the resulting slip surface must be the

same as the derived ones. Also, the boundary conditions on the slip surface are the same.

Experimentally $\alpha_0 = \pi/4 + \phi/2$, see Juran and Christopher, (1989) [13]. Thus, from the

first slip surface in Eq. 28 and 29, $-\delta_n$ will have higher values than ϕ, since $\delta_0 = 0$. This

is expected since the shear can be taken by the reinforcements. The second slip surface

will finish at a point similar to the front face, since that portion of the wall can be taken as

a surcharge on a layer of reinforcements. Thus the tension in these reinforcements takes

the lateral load leaving the upper surface at the surcharge area to start anew. Thus,

$\alpha_m = \pi/4 + \phi/2$. At this point δ_m will have a value similar to δ_n. Thus, from there on it

can be considered similar to an incipient shear at zero deflection, and the slip surfaces

will repeat. When integrating over all the slip surfaces, the final horizontal and vertical

forces to the top of the wall will not be zero; they represent the total horizontal and

vertical forces in the reinforcements. In both cases, the friction on the bottom of the slices

is fully mobilized causing an active slip surface. Even though the equations come out the

same, due to the variational function, the location of the forces are not in the same place.

To find the location of ΣdE_x and ΣdE_y in a reinforced earth mass, it is necessary to take

moments of the slices. Thus $M_x = \Sigma y dE_x$ and $M_y = \Sigma x dE_y$. By integrating over all the slip

surfaces, to the top of ground, the moments can be obtained, thus the location of the

forces.

When comparing with an experiment found by Juran, Beech, and De Laure[12] this gives

a good result. Their experiment gave data for a slip surface for a rigid inclusion
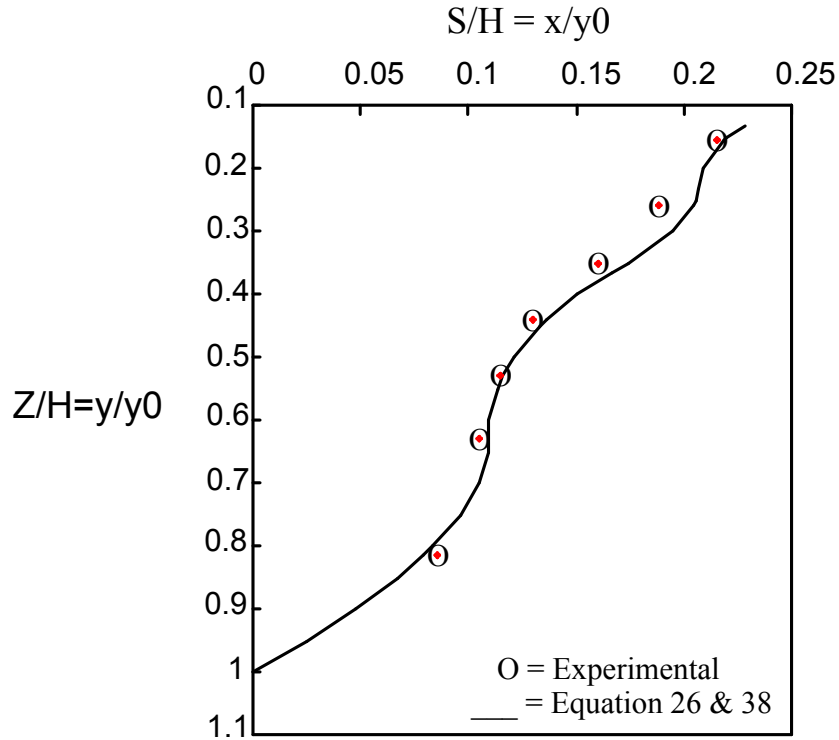
FIG. 5 Comparison of Slip Surface with Experiment (Juran et al.1984) for $\phi = 35$

(a relatively rigid polystyrene) soil nailed wall. The rigid polystyrene strips failed because of excessive bending. The failure surface was observed in the soil using colored sand coinciding with the location of the breakage points in the reinforcements. However, when the failure is induced by excessive nail bending, the breakage points are located at a certain distance behind the failure surface observed in the soil. It is expected that in a rigid soil nailed wall the slip surface in front of the breakage points is that of K_0. Fig. 5 shows an excellent result (0.7% Ave error or 0.7cm for H = 100cm) for $\phi = 35$ deg using Eq. 26 and 38 repeatedly. Note: the total x distance from the face of the wall to the slip surface on the top surface is equal to $x_m(1 + \sin\phi)$, where x_m is that of Eq. 39.
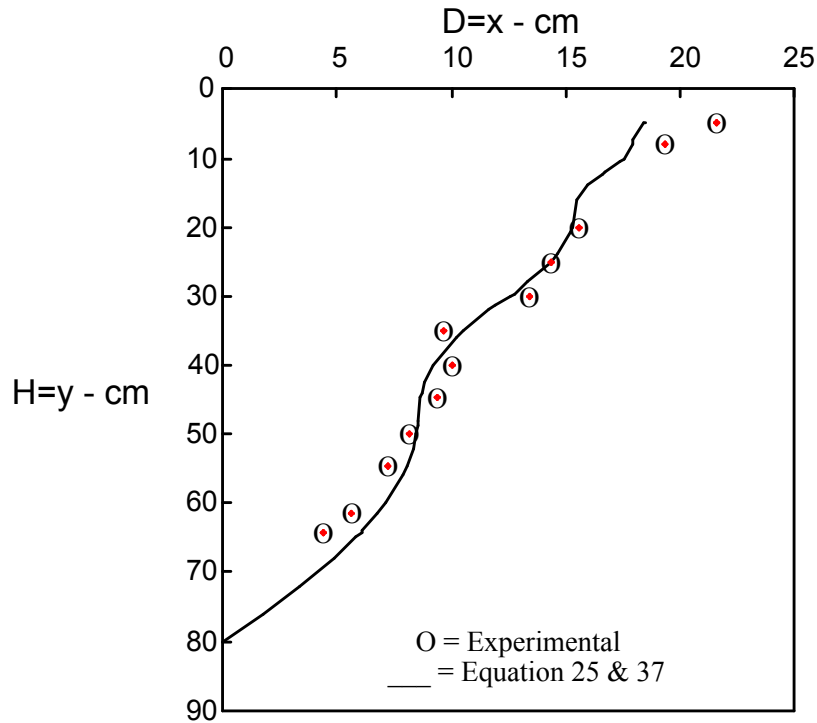
FIG. 6 Comparison of Slip Surface with Experiment (Juran et al. 1989)

(Model No. 3 - End of Construction) $\phi = 40$ and $y_0 = 80$ cm

Juran and Christopher[13] did a laboratory model study on geosynthetic reinforced soil retaining walls. The soil used in the study was a fine Fontainbleau sand (poorly graded, average grain diameter 0.1 mm) with $\phi = 40$. Colored sand was used to detect the failure surface in the soil. Three different types of geosynthetic reinforcing materials were used: Woven polyester strips; non-woven geotextiles; and plastic grids. The results on the tension forces measured in the woven geotextile strips correspond fairly well to those estimated, assuming that the soil is at K_0 state stress. In his third model wall (Model No. 3) the initial failure surface at end of construction was observed to be quite different from
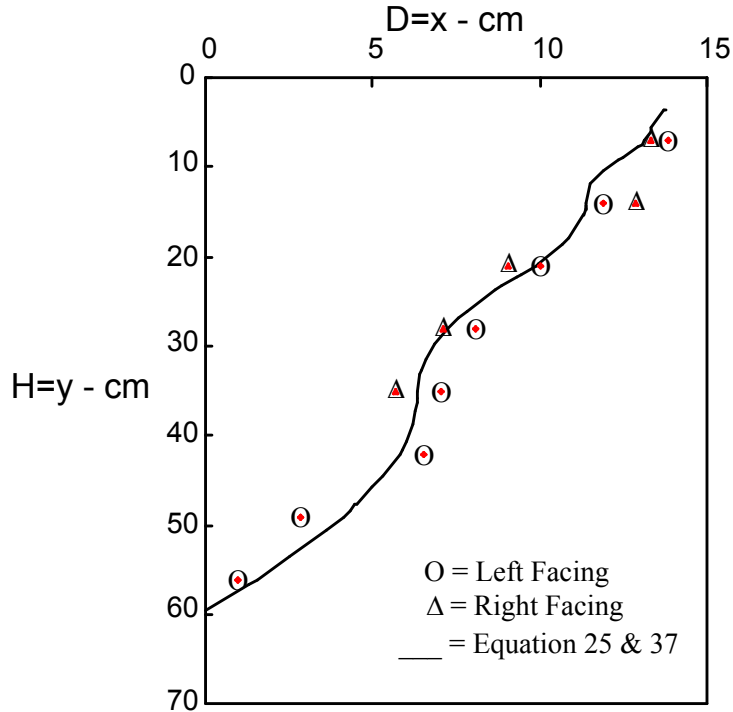
FIG. 7 Comparison of Slip Surface with Experiment (Juran et al. 1989)

(Model No. 7 - with Plastic Grids) $\phi = 40$ and $y_0 = 59.5$ cm

Coulomb's failure plane, whereas the final one (failure after 12hr) corresponds fairly well

to Coulomb's failure plane. It is expected that the initial failure surface at end of

construction will correspond to K_0 failure surface. Fig. 6 shows an excellent result (1.3%

Ave error or 1.05cm for H = 80cm) for $\phi = 40$ deg, where the angle $\phi = 40$ gives the exact

Coulomb's failure plane observed after 12hr. The results on the tension forces measured

in the non-woven geotextiles for low overburden correspond fairly well to those

estimated, assuming that the soil is at K_a state stress. However, as the overburden stress

increases, the reinforcement material seems to undergo a strain hardening phenomenon

and the tension forces in the reinforcements approach those predicted, considering a K_0

state of stress in the soil. The initial failure surface is expected to be of a K_0 slip surface but it was not recorded. However, it was mentioned in Juran, Ider, and Farrag[14] to be an inclination of 75 to 78 degrees; which is expected for a K_0. The result on the tension forces measured in the plastic grid are close to those predicted, assuming that the soil is at K_0 state stress. The initial and final surface is quite different from the Coulomb failure surface. This is expected since rigid inclusions were used. Fig. 7 shows excellent result (1.12% Ave error or 0.66cm for H = 59.5cm) for ϕ = 40 deg.

Overconsolidation of sand

When the present effective overburden pressure is the maximum pressure to which the soil has been subjected at any time in its history, the deposit is referred to as normally consolidated. A soil deposit that has been fully consolidated under a pressure larger than that of the present overburden is called overconsolidated. The K_0 of Eq. 8 and 46 is referred to as normal consolidation because the weight used in the derivation is the existing weight, and no prehistoric weight causing locked-in stresses were used. To achieve overconsolidation forces, locked-in horizontal forces must enter the equations and be considered on each slice. For the purpose of demonstration of dependencies, a one-dimensional approach will be used. Consider the structural beam in Fig. 8.
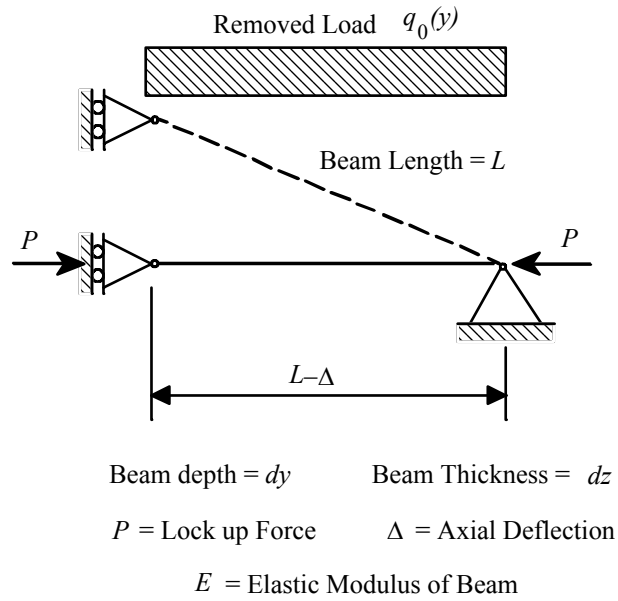
FIG. 8 - Locked-in Force in a Beam

The uniform load $q_0(y)$ has deflected the beam axially to a horizontal position. Then the load $q_0(y)$ is removed from the beam. If the beam cannot go completely back to its original position, the result is a locked-in force P. Writing the force P in terms of deflection yields: $P = dzdy\Delta E / L$. When considering that the locked-in force in the structural beam corresponds to locked-in forces in soil, E can be replaced by the soil spring modulus E' due to the intensity of the contact pressure. Δ can be replaced by the change in unit weight from loose to dense: $L / (L - \Delta) = \gamma_L / \gamma_D$, $\Delta = (1 - \gamma_L / \gamma_D)L$, where γ_L is the loose unit weight and γ_D is the dense unit weight after load removal (or rebound). Thus, $P = dzdyE'(1 - \gamma_L / \gamma_D)$. Terzaghi, (1955) [24], recommended values for cohesiveless soil spring constants $E' = n_h y$. Where n_h is the subgrade modulus, and y is the depth. His tests were done under compression loading and n_h has a range from 7-56 Tons/ft³ (or 0.22-1.79 kg/cm³) for dry moist sand, and 4-34 Tons/ft³ (or 0.13-1.09 kg/cm³) for submerged sand. Thus, the compressive force in the soil can be estimated, and

$P_{compressive} = n_h(1 - \gamma_L / \gamma_D)ydzdy$. To find the necessary locked-in stresses to be used along with the at rest forces, one must find the expansion force. Since soil is not elastic, the compression force is not equal to the expansion force and it is much greater. Consequently, the compression force can be reduced by using the expansion to compression voids ratio. Thus the expansion locked-in force becomes

$$P_{expansion} = n_h \frac{e_e - e_c}{e_i - e_c}\left(1 - \frac{\gamma_L}{\gamma_D}\right)ydzdy \quad \text{...} \quad (52)$$

So, e_e is the expansion voids ratio at rebound or at load removal at γ_D, e_c is the compressed voids ratio at full load, and e_i is the initial voids ratio at loose state γ_L. Now, if the prehistoric surcharge is $q_c(y)$, then the compressive horizontal force is $K_0 q_c(y)dydz$. However, not all of the surcharge can be used since some expansion in the soil will occur after the removal of the surcharge. Thus, at compression to γ_D the horizontal locked-in force can be taken as $q(y)dydz$, where $q(y)$ is to be determined. Equating this force with the expansion force of Eq. 52 yields

$$q(y) = n_h \frac{e_e - e_c}{e_i - e_c}\left(1 - \frac{\gamma_L}{\gamma_D}\right)ydy \quad \text{...} \quad (53)$$

In order to include $q(y)$ in the derivation, the forces must be split into loose condition plus the locked-in force of Eq. 53. This is necessary since the estimated Δ was for loose to dense sand. Additionally, from Fig. 8, the overconsolidation force is to be considered only in the horizontal direction. Thus, the resultant dE_x and dE_y for Eq. 2, 3, and 4 becomes:

$$dE_x = \frac{\tan(\alpha - \phi)}{1 + \tan\delta \tan(\alpha - \phi)} \frac{d\overline{w}}{\tan\alpha} + n_h \frac{e_e - e_c}{e_i - e_c}\left(1 - \frac{\gamma_L}{\gamma_D}\right)y\,dy \quad\text{.................................. (54)}$$

$$dE_y = \frac{\tan(\alpha - \phi)\tan\delta}{1 + \tan\delta \tan(\alpha - \phi)} \frac{d\overline{w}}{\tan\alpha} \quad\text{.. (55)}$$

$$dW = -\gamma_L\left[\frac{(y - dy) + y}{2}\right]\frac{dy}{\tan\alpha} = \frac{d\overline{w}}{\tan\alpha} \quad\text{... (56)}$$

When performing the boundary analysis, dE_x in Eq. 6 must have the additional term in

Eq. 54, and so the resulting boundary condition remains the same. Furthermore, when

performing the same analysis for obtaining δ and variational analysis the result leads to

the same slip surfaces. Therefore, the resulting coefficient K_{0c} for over consolidation

becomes:

$$K_{0c} = K_0 + \frac{n_h}{\gamma_L}\frac{e_e - e_c}{e_i - e_c}\left(1 - \frac{\gamma_L}{\gamma_D}\right) = K_0 + \frac{n_h}{\gamma_D}\frac{e_e - e_c}{e_i - e_c}\left(\frac{\gamma_D}{\gamma_L} - 1\right) \quad\text{................................. (57)}$$

$$\tan\delta_{0c} = \frac{K_0}{K_{0c}}\tan\delta_0 \quad\text{... (58)}$$

Where, K_0 is of Eq. 46 (with ϕ for loose sand), and δ_0 is of Eq. 47 (with ϕ for loose sand).

It is remarkable that ϕ has no influence on the additive term due to overconsolidation, and

γ_L and γ_D has the greatest influence. Let $k_h = (n_h / \gamma_D)[(e_e - e_c)/(e_i - e_c)]$. The term k_h is

approximately constant, since n_h is obtained by similar methods as the expansion to

compression deflection ratio. n_h varies with the density of material, and so are the

required voids ratios. The variation of γ_D from γ_L is in the range from 0 to 6%. So, γ_D can

be considered approximately constant. Thus, the term k_h can be considered constant. On

the other hand, the incipient shear angle is reduced per Eq. 58. This is expected, since the failure wedge will be reached sooner due to overconsolidation. It is important to keep in mind that Eq. 57 and Eq. 58 were derived to investigate dependencies for a very complex problem. However, it is of merit to compare with experimental results. Sherif et. al., (1985) [22], showed that the variation of the additional term to K_0(loose) is linearly dependent with γ_D/γ_L. Their experimental results for dry Ottowa Sand gave the value for $k_h = 5.5$. When using an average value $n_h = 27$ tcf and $\gamma_D = 100$ pcf (from Sherif et. al.) it yields $(e_e - e_c)/(e_i - e_c) = 5.5/540 = 0.01$. This is a very reasonable expansion to compression deflection ratio in sand. Thus it appears that Eq. 57 and 58 are valid for the conditions described above. When repeating the analysis in a higher dimension, as in a circular plate or a square plate with plane strain analysis, new equations can be derived. Thus, $P = dzdy\Delta E/[L(1+\nu)(1-2\nu)]$, where ν is Poisson's ratio. From the volume ratio of before and after, $\Delta/L = 1 - \sqrt{\gamma_L/\gamma_D}$ giving $K_{0c} = K_0 + 10.6\left[\gamma_D/\gamma_L - \sqrt{\gamma_D/\gamma_L}\right]$, where ν was replaced by .3 for sand and $k_h = 5.5$ (from Sherif et. al.). When comparing numerically this equation with Sherif's equation the results is of no significance in the difference in the additive term to K_0 where $1 < \gamma_D/\gamma_L < 1.07$.

Clay Analysis

Preliminary analysis indicates when the cohesion "c" is involved in the equations, mathematical harmony is difficult to achieve. It indicates that c will influence the slip

surfaces, K_0, and the incipient shear angle. If the solution is to be done for only cohesion with $\phi = 0$, the boundary angle becomes 45 degrees, and the variational equation gives a 45 degrees line as the slip surface. This is an indication that if cohesion is added it will influence the solution more toward a line than a curve. Thus, a reasonable approximation of the solution for the normal consolidating clay can be obtained by using similar procedures as in Eq. 8. Table 1 shows the difference between Eq. 8 (Jáky's Eq. 1) and the derived Eq. 46 ranges from 0 to 8%. This difference can always be handled with a safety factor similar to the one proposed by Handy, (1985) [8]. When adding the cohesion c on the bottom of the slice, while keeping it in an upward direction and separate from dQ in Fig. 3-b, the resultant dE_x and dE_y for Eq. 2, 3, and 4 becomes:

$$dE_x = \frac{\gamma \overline{dw} \tan(\alpha - \phi) \cot \alpha + c[\tan(\alpha - \phi) + \cot \alpha]dy \pm c' \tan(\alpha - \phi)dy}{1 + \tan \delta \tan(\alpha - \phi)} \quad \text{.........................} \quad (59)$$

$$d\overline{E}_y = dE_y \pm c'\,dy = dE_x \tan \delta \quad \text{..} \quad (60)$$

where c' is the adhesion on the slice's boundary, c' dy is taken in front of the slice , and $d\overline{E}_y$ is the resultant vertical force separate from the adhesion so that the directional angle δ is separated from the adhesion to insure $|\delta| < \phi$. This can be seen by noting the cohesion on the bottom of the slice reduces dE_x and $d\overline{E}_y$ since it reduces dW. If assuming all α's greater than $\pi/4$, due to an active slip surface, then $d\overline{E}_y$ will reduce more than dE_x. Thus $d\overline{E}_y / dE_x$ will be lower than if there was no cohesion. Hence, $|\delta| < \phi$ as long as the adhesion is separated.

For the boundary condition Eq. 59 is rewritten in terms of dE_x, dE_y, and dx:

$$-dE_y = -\gamma y\, dx + dE_x \cot(\alpha - \phi) + c\, dx[\tan\alpha + \cot(\alpha - \phi)] \quad\text{... (61)}$$

dE_x at the boundary is the at rest force and it can be taken as $-(\gamma K_0 y\, dy - \overline{K}_0 c\, dy)$, where $\overline{K}_0$ is the additional term for cohesion. Thus Eq. 61 becomes:

$$-dE_y = -\gamma y\, dx + (K_0 y - \overline{K}_0 c)dx \tan\alpha \cot(\alpha - \phi) + c\, dx[\tan\alpha + \cot(\alpha - \phi)] \quad\text{....................... (62)}$$

Minimizing the force $-dE_y$ in Eq. 62, $-\dfrac{dE_y}{d\alpha}\bigg|_{x=0 \text{ and } x=x_m} = 0$, yields $\alpha = \alpha_0 = \alpha_m = \pi/4 + \phi/2$.

Substituting in Eq. 59 $\tan(\alpha - \phi) = \tan(\pi/4 - \phi/2) = -\tan\phi + 1/\cos\phi$,

$\cot\alpha = \tan(\pi/4 - \phi/2)$, $c' = c$, $\delta = -\phi$, taking the adhesion at the back of the slice to be in the opposite direction of the incipient shear so that the minus sign of the $\pm$ sign applies, and integrating from y_0 to 0 yields the force:

$$E_0 \cos\delta_0 = \gamma \frac{y_0^{\,2}}{2}(1 - \sin\phi) - c y_0 \cos\phi \quad\text{... (63)}$$

Thus, the stress is

$$\sigma_h = \frac{dE_x}{dy_0} = \gamma y_0 (1 - \sin\phi) - c \cos\phi \quad\text{.. (64)}$$

The most remarkable conclusion in Eq. 64 is that K_0 for clay is not constant when using $\sigma_h / \sigma_v = \sigma_h / \gamma y$. Preliminary investigation indicates that even if the closed form solution is achieved the result is the same. But each term is still individualized by y_0. In consideration of the simplicity of Eq. 64, other notable remarks can be made: (1) The equation is consistent with soil mechanics equations with cohesion such as active pressure, passive pressure and bearing capacities, where the cohesion and the cohesionless terms are two separate terms and not mixed. (2) The distance to zero stress calculated in active condition is at $y_1 = 2c / \gamma \sqrt{K_a}$, and Eq. 64 gives one half this distance. This indicates that during a wall movement from at rest condition until an active condition the surcharge due to the tension zone increases by 1/2. This is also consistent with common sense, since one expects y_1 to be between zero, or no tension, and the active tension zone, the maximum tension zone. 1/2 is exactly the average value. (3) If considering the undrain shear strength S_u, the stress becomes $\sigma_h = \gamma y - S_u$, which is greater than the active condition $\gamma y - 2S_u$. This is expected from the at rest condition to be higher than the active condition for short-term loading. (4) When the ground is at rest, and due to gravity weight, tension must exist on top causing tension cracks from earthquake or any traction force. Comparing with elasticity, the elastic solution gives zero stress on top, which is contrary to physical evidence. Tension cracks exist in clay even in the at rest condition due to earthquake or any traction force. From these considerations, Eq. 64 offers a reasonable working formula for normally consolidated clay.

Comparison with Experimental value for Clay

Unfortunately, all the available tests did not account for cohesion. If considering

$$K_0 = \frac{\sigma_h}{\sigma_v} = 1 - \sin\phi - \frac{c}{\gamma y}\cos\phi,$$ the test will match depending on the load applied with σ_h.

Thus, if σ_h is high , so the overburden is high, then $c\cos\phi/\gamma y$ becomes a small number

and in this case $K_0 \cong 1 - \sin\phi$ matches Mayne and Kulhawy, (1982) [17]. On the other

hand, Brooker and Ireland, (1965) [2], recommended $K_0 = 0.95 - \sin\phi$ for five different

kinds of clay. This may be an indication that c was high for these clays and the term

$c\cos\phi/\gamma y$ reduces the overall K_0. For example: if $\gamma y = 94$psi, for a high overberden, $c =$

5psi and $\phi = 20^o$, it gives $c\cos\phi/\gamma y = 0.05$ for the clay used in their experiments. This

cohesion to initial stress ratio accounts for the overall reduction in K_0. In any case, Eq. 64

suggests new verifications tests are necessary for clay. This becomes a primary

recommendation of this manuscript.

Overconsolidation in Clay

If setting the $c = 0$ in the closed form solution for clay (if obtained), the results must be

the same as the equations for cohesionless soil. Thus, the equation of overconsolidation

of sand, Eq. 54, must be modified for clay, where $E' \neq n_h y$. Substituting and integrating

from y_0 to 0 over all sets of slip surfaces for cohesionless terms, and integrating over y_0

to y_2 for the overconsolidating term, yields

$$\int dE_x = \gamma_L K_0 \frac{y_0^2}{2} + E' \frac{e_e - e_c}{e_i - e_c}\left(1 - \frac{\gamma_L}{\gamma_D}\right)(y_0 - y_2) \quad\text{.. (65)}$$

where y_2 is the distance from the top of surface where overconsolidation stress starts. Adding back the cohesion term to the equation, and expressing it as stress as in Eq. 64, yields

$$\sigma_h = \gamma_L(1 - \sin\phi)y - c\cos\phi + E' \frac{e_e - e_c}{e_i - e_c}\left(1 - \frac{\gamma_L}{\gamma_D}\right) \quad\text{.. (66)}$$

Note: the additive term in Eq. 66 for overconsolidation is independent of ϕ and y, predicting a constant value throughout the ground, when higher than the cohesion term. This constant value is very reasonable for clay when E' is constant with depth. However, in practice the additive term for overconsolidation should start at a distance at least greater than y_1 (the distance of tension in the ground). This is necessary since locked-in stresses cannot occur on the top surface.

When repeating the analysis in a higher dimension, as in a circular or square plate with plane strain analysis, equation 66 is replaced by:

$$\sigma_h = \gamma_L(1 - \sin\phi)y - c\cos\phi + E' \frac{e_e - e_c}{e_i - e_c} \frac{1}{(1 + \nu)(1 - 2\nu)}\left(1 - \sqrt{\frac{\gamma_L}{\gamma_D}}\right) \quad\text{............................ (67)}$$

Eq. 67 is preferred than Eq. 66 since it is more realistic.

If defining $\text{OCR} = (\sigma_0 + \sigma_1)/\sigma_0 = 1 + \sigma_1/\sigma_0$, where σ_0 is the initial stress $\gamma_L y$, and $\sigma_0 + \sigma_1$ is the initial plus the overburden stress, then the additive term can be expressed as:

$$q(y) = \frac{e_e - e_c}{e_i - e_c} K_0 \sigma_1 = \frac{e_e - e_c}{e_i - e_c}(\text{OCR} - 1)\sigma_h \quad\text{..} \quad (68)$$

where σ_h is of Eq. 64. Substituting Eq. 68 in Eq. 66 to replace the additive term yields:

$$\sigma_h = \gamma_L(1 - \sin\phi)y - c\cos\phi + \left[\gamma_L(1 - \sin\phi)y - c\cos\phi\right]\left(\frac{e_e - e_c}{e_i - e_c}\right)(\text{OCR} - 1) \quad\text{..................} \quad (69)$$

and

$$K_{0c} = \left[1 - \sin\phi - \frac{c\cos\phi}{\gamma_L y}\right] \cdot \left[1 + \frac{e_e - e_c}{e_i - e_c}(\text{OCR} - 1)\right] \quad\text{..} \quad (70)$$

Eq. 70 indicates K_{0c} varies linearly with OCR for a constant expansion to compression deflection ratio independent of OCR, and for a given initial stress $\gamma_L y$. If comparing Eq. 70 with Brooker and Ireland, (1965) [2] for five clays, four clays gives a secant slope of 0.075 (Chicago Clay, London Clay, Goose Lake Flour, and Weald Clay), and one clay gives 0.042 (Bearpaw Shale). This gives an expansion to compression deflection ratios of 0.13, 0.11, 0.14, 0.12, and 0.06 respectively. This is a very reasonable expansion to compression deflection ratio $(e_e - e_c)/(e_i - e_c)$ for clay. Thus, Eq. 70 appears to be a reasonable approximation.

Conclusion

The mystery of why Jáky's equation agrees with experimental data is resolved.

Furthermore, the established incipient shear failure mechanism in obtaining K_0 should

satisfy many engineers and scholars who believe K_0 should not be related to failure

parameters (ϕ & c), since no failure criterion seem to appear in the at rest condition.

Additionally, the incipient shear failure mechanism offers solutions for other problems

besides K_0. Variational method has been used in the analysis to obtain a closed form

solution for K_0 for sand. The methods are classical and conventional and only practical

assumptions were used. The extremum condition indicates the existence of two slip

surfaces back to back. If using a line approximation with the same boundary condition the

result is identical to Jáky's equation. On the other hand if using the closed form equation,

the result is a slightly higher value for K_0. The derived K_0 is in excellent agreement with

experimental results and matches safety factor recommendations for Jáky's K_0. The

corresponding slip surfaces are in excellent agreement with rigid reinforced earth walls.

The analysis was carried out further to establish physical criterion and equations for

overconsolidating sand. The result is in fair agreement with experiments and shows the

different parameters influencing the locked-in forces. Finally, the analysis is repeated for

deriving K_0 for normal and overconsolidating clay. The slip surface used is approximate,

but gives a reasonable approximation for K_0. The results are in good standing with

experiments. The derived equations were used to determine the tension zone distance in

clay. This distance is one half the active distance and is very reasonable. In general, in

clay, K_0 is not constant with depth as apparent in the results. The paper offers the real K_0

with a high confidence factor. However, further experiments and research are necessary

to verify the many consequences of using variational methods. The following are recommended experiments and research:

1) Experiment to verify the tension zone distance in clay.

2) Experiment to verify the effect of c in K_0 in clay.

3) Further research is needed in overconsolidating clay since the additive term related to OCR is shown experimentally non-linear indicating the expansion to compression deflection ratio is dependent on OCR.

The derivation can be readily extended for a slanted wall with a sloped soil on surface. This in turn prepares the way for dynamic analysis. The theory can also be extended for multi-layers of different soils in the ground. The equations derived in this manuscript are expected to be used in a wide variety of engineering practice.

Appendix I.-References

1.   Bishop, A. W. (1955). "The Use of Slip Circle in the Stability Analysis Analysis of Slopes," *Géotechnique*, London, England, Vol. 5, No. 1, pp. 7-18.

2.   Brooker, E. W., and Ireland, H. O., (1965). "Earth Pressures at Rest Related to Stress History," *Canadian Geotechnical Journal*, National Research Council, Ottaws, Ontario, Vol. II, No. 1, pp. 1-15.

3.   Coulomb, Charles Augustin (1776). "Essai sur une application des règles de maximis et minimis à quelques problèmes de statique relatifs à l'architecture," *Mem. Div. Savants,* Acad. Sci., Paris, Vol. 7.

4.   D'Appolonia, D. J., Lambe, T. W., and Poulos, H. G. (1971). "Evaluation of Pore Pressures Beneath an Embankment," *Journal of Soil Mech. and Foundations Div.*, ASCE, 97(SM6), pp. 881-867.

5.   DeLory, F. A., and Salvas, R. J. (1969). "Some Observations on the Undrain Shearing Strength Used to Analyze a Failure," *Can. Geotech. J.*, 6(2), pp. 97-110.

6.   Donaghe, R. T., and Townsend, F. C. (1978). "Effects of Anisotropic Versus Isotropic Consolidation in Consolidated Undrained Triaxial Compression Tests of Cohesive Soil," *Geotech. Test. J.*, ASTM, 1(4), pp. 173-189

7.   Fang, Y-S, and Ishibashi, I. (1986). "Static Earth Presures with Various Wall Movements," *J. of Goetech. Engrg.*, ASCE, 112(3), pp. 317-333

8.   Handy, R. L. (1985). "The Arch in Soil Arching," *J. Geotech. Engrg.*, ASCE, 111(3), pp. 302-318.

9. Handy, R. L. (1983). Discussion of "K_0 - OCR Relationships in Soil," by P. W. Mayne, and F. H. Kulhawy, *J. of Geotech. Engrg.*, ASCE, (109)6, pp. 862-864

10. Jáky, J. (1944). "A Nyugalmi Nyomás Tényezóje," *Magyar Mérnok es Epitész Egylet Kozlonye (Journal of the Society of Hungarian Architects and Engineers)*, pp. 355-358

11. Jáky, J. (1948). "Pressure in Silos," *Proceedings of the Second International Conference on Soil Mechanics and Foundation Engineering*, Vol. I, pp. 103-107

12. Juran, I., Beech, J., and De Laure, E. (1984). "Experimental Study of the Behavior of Nailed Soil Retaining Structures on Reduced Scale Models," *Proc. Int. Symp. In-Situ Soil and Rock Reinforcement*, Paris, France.

13. Juran, I., and Christopher, B. (1989). "Laboratory Model Study on Geosynthetic Reinforced Soil Retaining Walls," *J. Geotech. Engrg.*, ASCE, 115(7), pp. 905-926.

14. Juran, I., Ider, H. M., and Farrag., K. (1990). "Strain Compatibility Analysis for Geosynthetics Reinforced Soil Walls," *J. Geotech. Engrg.*, ASCE, 116(2), pp. 312-329.

15. Khera, R. P., and Krizek, R. J. (1967). "Strength Behavior of an Anisotropically Consolidated Remolded Clay, " *Highway Research Rec.*, 190, pp 8-18.

16. Koutsoftas, D. C., and Ladd, C. C. (1985). "Design Strength for an Offshore Clay," *J. Geotech. Engrg.*, ASCE, 111(GT3), pp. 337-355.

17. Mayne, P. W., and Kulhawy, F. H. (1982). K_0 - OCR Relationships in Soil," *J. of Geotech. Engrg.*, ASCE, (108)6, pp. 851-872.

18. Mesri, G., and Castro M. A. (1987). "C_α/C_c Concept and K_0 during Secondary Compression," *J. of Geotech. Engrg.*, ASCE, (113)3, pp. 230-247.

19. Nakase, A., and Kamei, T. (1983). "Undrained Shear Strength Anisotropy of Normally Consolidated Cohesive Soils," *Soils Found.*, 23(1), pp. 91-101.

20. Nakase, A., and Kobayashi, M. (1971). "Change in Undrained Shear Strength of Saturated Clay Due to Rebound," *Proceedings of the 4th Asian Regional Conference on Soil Mechanics and Found. Engineering*, Bangkok, Thailand, Vol. 1, pp. 147-150

21. Sherif, M. A., and Fang, Y. S. (1984). "Dynamic Earth Pressures on Walls Rotating about the Top," *Soil and Foundations, Japanese Society of Soil Mechanics and Foundation Egineering*, Vol. 24, No. 4, pp. 109-117.

22. Sherif, M. A., Fang, Y. S., and Sherif, R. I. (1984). "K_a and K_0 Behind Rotating and Non-Yeilding Walls," *J. of Geotech. Engrg.*, ASCE, (110)1, pp. 41-56.

23. Sherif, M. A., Ishibashi, I., and Do Lee, Chong (1982). "Earth Pressures Against Rigid Retaining Walls," *J. of Geotech. Engrg.*, ASCE, (108)5, pp. 679-695.

24. Terzaghi, K. (1955). "Evaluation of Coefficients of Subgrade Reaction," *Geotechnique*, Vol. 5.

25. Terzaghi, K. (1941). "General Wedge Theory of Earth Pressures," *Trans. Am. Soc. Civil Eng.* No.106, Vol. 67, pp. 68-80

26. Terzaghi, K. (1934). "Large Retaining-Wall Tests," *Engineering News-Record*, Vol. 112, pp. 136-140, 259-262, 316-318, 403-406, 503-508.

27. Timoshenko, S. P., and Goodier, J. N. (1970). Theory of Elasticity, McGraw-Hill Book Company Inc., New York, N. Y., 3rd Edition, p. 97.

28. Tschebotarioff, G. P., (1953). Soil Mechanics Foundations and Earth Structures, McGraw-Hill Book Company Inc., New York, N. Y., p. 256.

29. Weinstock R., (1974), Calculus of Variations With Applications to Physics and

Engineering, Dover Publications, Inc., New York, N. Y., pp. 22-25, and pp. 36-40.

Appendix II.- Notation

   The following symbols are used in this paper:

α = angle of the failure wedge, or of failure a slice, with the horizontal;

α_0 = slice wedge angle with the horizontal at start of first slip surface at $x = 0$;

α_m = slice wedge angle with the horizontal at end of second slip surface;

α_n = slice wedge angle at end of first slip surface or start of second slip surface;

c = cohesion in clay;

c' = adhesion on the slice boundary;

D   = x - term used in experimental paper by others;

Δ = axial deflection of a beam;

δ = Coulomb friction, directional frictional angle between dE_x and dE_y;

δ_0 = directional angle at first slice boundary at $x = 0$ = incipient shear angle;

δ_i = directional angle at slice boundary at x;

δ_m = directional angle at last slice boundary at $x = x_m$ = incipient shear angle;

δ_n = directional angle at slice boundary at $x = x_n$;

E = elastic modulus of beam;

E' = spring modulus of soil;

E_0 = directional force of first slice boundary at $x = x_0$;

E_h = horizontal force at rest;

ΔE_h = change in horizontal force;

E_i = directional force of slice boundary at x;

E_m = directional force of last slice boundary at $x = x_m$;

E_n = directional force of slice boundary at $x = x_n$;

dE_x = slice horizontal resultant force;

dE_y = slice vertical resultant force;

$d\overline{E}_y$

  = resultant of vertical force on a slice separate from slice adhesion;

e_c = compressed void ratio at full load;

e_e = expansion void ratio at rebound or at load removal;

e_i = initial voids ratio at loose state;

F = immobile friction force;

ΔF = change in immobile friction force;

ϕ = angle of internal friction of soil;

γ = soil unit weight;

γ_D = unit weight of soil at dense state or at rebound state;

γ_L = unit weight of soil at loose state or initial state;

H   = y - term used in experimental paper by others;

h = mathematical coefficient in the slip surface equations;

h' = mathematical coefficient in the slip surface equations related to h;

i = integer counter;

K = coefficient of lateral earth pressure or lateral stress ratio;

K_0 = at rest earth pressure coefficient;

$\overline{K}_0$ = additive term for the coefficient of earth pressure for cohesion;

K_{0c} = coefficient of lateral earth pressure at rest for overconsolidation;

K_1 = dimensionless coefficient representing a term in an equation;

K_a = active earth pressure coefficient;

K_p = passive earth pressure coefficient;

k_h = $(n_h / \gamma_D)[(e_e - e_c) / (e_i - e_c)]$;

L = length of beam;

m = integer;

M_x = total moment of the horizontal forces of all the slices;

M_y = total moment of the vertical forces of all the slices;

ν = Poisson's ratio;

N = normal force;

ΔN = change in normal force;

n = integer;

n_h = subgrade modulus of sand;

OCR = overconsolidation ratio;

P = locked-in force in a beam;

P_1 = downward shear force on wall;

P_2 = upward shear force on wall;

dQ = reactive force on bottom of failure wedge or slice to maintain equilibrium;

q = uniform surcharge pressure;

$q(y)$ = unknown horizontal stress for overconsolidation;

$q_0(y)$ = uniform surcharge load that causes locked-in force in a beam;

$q_c(y)$ = prehistoric surcharge;

$\mathfrak{R}$ = calculus of variation function of mixed variables representing the integrand;

r = correlation number;

S/H = x/y_0 - term used in experimental paper by others;

S_u = undrain shear strength for short term loading;

σ_0 = initial stress = $\gamma_L y$ - in overconsolidations;

σ_1 = overburden stress in overconsolidations;

σ_h = the horizontal stress in soil;

σ_v = the vertical stress in soil;

T = incipient shear;

W = vertical force from weight of wedge;

dW = weight of slice;

$d\overline{w}$ = weight of slice times tanα;

Ω = dimensionless variable = x/y_0;

x = coordinate x-axis;

dx = width of slice's wedge;

x' = dx/dy;

x_m = distance to tip of second slip surface;

ψ = dimensionless variable = y/y_0;

y = coordinate height at y-axis;

dy = height of slice's wedge;

y' = dy/dx;

y_0 = height of wall or start of first slip surface at $x = 0$;

y_1 = tension zone distance in clay;

y_2 = distance from the top surface to where the overconsolidation stress starts;

y_m = height distance at end of second slip surface;

y_n = height distance at end of first slip surface or start of second slip surface;

Z/H = y/y_0 - term used in experimental paper by others;

dz = beam thickness;

Appendix III.- Numerical Check

With the advent of software technology, numerical differentiation and integration easily has become easier. Algebra can be checked from one equation to a reduced equation by numerical substitution to give identical values. Many software programs are available to do the checking. All of the derived equations were checked with MATHCAD *on a personal computer, including starting with the variational (Euler equation). The following constants' relations are necessary if the reader needs to double-check the writer:*

Eq. 22 .... $h' = -\dfrac{h}{2\gamma \sin\phi \cos\phi};$

and

Eq. 34 .... $h' = \dfrac{h}{2\gamma \sin^2 \phi}$.

Note: when using Sherif's expression their recommendations were to use γ_D and $K_0 =$ 1 - $\sin\phi$ for calculating the forces and the stresses. This effects the comparison slightly. Analysis shows the average $k_h = 5.87$ instead 5.5 in the region $32 < \phi < 44$ degrees and $1.03 < \gamma_D/\gamma_L < 1.07$. The analysis used K_0 from Eq. 46 and used γ_L in calculating the forces and the stresses.